Biomechanical Changes After LASIK Flap Creation Combined With Rapid Cross-Linking Measured With Brillouin Microscopy

J. Bradley Randleman, MD; Johnny P. Su, PhD; Giuliano Scarcelli, PhD

ABSTRACT

PURPOSE: To evaluate the biomechanical changes occurring after LASIK flap creation and rapid corneal cross-linking (CXL) measured with Brillouin light microscopy.

METHODS: Porcine eyes (n = 11) were evaluated by Brillouin light microscopy sequentially in the following order: virgin state, after LASIK flap creation, and after rapid CXL. Each eye served as its own control. Depth profile of the Brillouin frequency shift was computed to reveal the depth-dependent changes in corneal stiffness.

RESULTS: There was a statistically significant reduction of Brillouin shift (reduced corneal stiffness) after LASIK flap creation compared to virgin corneas across total corneal thickness (-0.035 GHz, P = .0195) and within the anterior stromal region (-0.104 GHz, P = .0039). Changes in the central (-0.029 GHz, P = .0391) and posterior (-0.005 GHz, P = .99) stromal regions were not significant. There was a small increase in Brillouin shift after rapid cross-linking that was not statistically or clinically significant across total corneal thickness (0.006 GHz, P = .4688 for any specific stromal region; 0.002 to 0.009 GHz, P > .46 for all).

CONCLUSIONS: LASIK flap creation significantly reduced Brillouin shift in the anterior third of the stroma in porcine eyes. Rapid corneal cross-linking had no significant effect on Brillouin shift after LASIK flap creation in porcine eyes. With further validation, non-contact, non-perturbative Brillouin microscopy could become a useful monitoring tool to evaluate the biomechanical impact of corneal refractive procedures and corneal cross-linking protocols.

[*J Refract Surg.* 2017;33(6):408-414.]

L ASIK induces biomechanical weakening of the cornea as a consequence of flap creation and excimer laser ablation. This typically has minimal long-term impact on corneal function or integrity, but in some circumstances it may lead to treatment regression, and ectasia can occur after LASIK in susceptible patients.[1] Extensive efforts have been undertaken to identify these susceptible eyes preoperatively, with some parameters clearly recognizable and others still under investigation.[2,3] Although the biomechanical reduction after flap creation is assumed, limited data exist to confirm or quantify this change.[4,5]

Corneal cross-linking (CXL) has been proven effective in strengthening the cornea using both in vivo and in vitro testing.[6,7] Clinically, this results in halting the progression of keratoconus and ectasia after LASIK, with progressive corneal flattening to varying degrees. A variety of different cross-linking protocols use varying combinations of irradiance time and energy to maintain total fluence. Initial studies used the standard (or Dresden) protocol (3 mW/cm^2 for 30 minutes, total fluence 5.4 J/cm^2),[6] whereas accelerated protocols have used power up to 30 mW for durations as short as 3 minutes with varying fluences and protocols.[8,9] These protocols induce varying degrees of corneal flattening that in many cases is progressive over many years.

Recently, modified rapid or accelerated protocols for CXL in combination with LASIK have been proposed to improve the biomechanical integrity of the post-LASIK cornea (herein

termed rapid CXL).[10] If successful, this process could theoretically reduce refractive regression and potentially reduce the incidence of postoperative ectasia. Because the progressive flattening typical for regular CXL protocols would be undesirable to combine with LASIK (it would negatively affect the refractive outcome), modified protocols have been proposed to induce a lesser cross-linking effect. Results to date have been mixed in terms of efficacy and safety.[11,12-14] Further, there has been limited research published regarding the potential biomechanical impact of rapid CXL. Kanellopoulos et al.[10] found increased stress and shear modulus and increased resistance to enzymatic degradation after rapid CXL in human donor corneas using ex vivo transverse biaxial resistance measurements. We are not aware of any other basic research in this area.

Porcine eyes have been used to evaluate CXL efficacy since the inception of the technique.[15,16] Recently, Brillouin microscopy has been developed for mapping material elastic modulus in three dimensions with a high spatial resolution.[17-19] This optical technique is non-invasive and does not involve structural or mechanical deformation of the cornea, and is thus suitable for application in clinical settings. Brillouin microscopy was previously applied to investigate the biomechanical properties of the cornea in patients with keratoconus[20,21] and after various riboflavin-mediated CXL procedures.[22-24] Keratoconic corneas had lower Brillouin shift (ie, lower elastic modulus and decreased mechanical stability). Brillouin measurements showed a much larger separation between normal and ectatic corneas than what the Ocular Response Analyzer (ORA) (Reichert Technologies, Inc., Depew, NY) measured on comparable samples.[25] After CXL, Brillouin corneal stiffness increased after epithelium-off CXL. The increase of Brillouin modulus was depth dependent, indicating that anterior stromal stiffening contributes the most to mechanical outcome. The findings were more pronounced than those found using the ORA in vivo.[26]

The purpose of this study was to evaluate the biomechanical effect of rapid CXL combined with LASIK flap creation using Brillouin microscopic imaging in porcine corneas.

MATERIALS AND METHODS

A total of 11 freshly enucleated porcine eyes were obtained from a local slaughterhouse. They were kept in ice during transportation until the start of the experiment. The experiment was completed within 8 hours after the pigs were killed. All corneas with intact epithelium were visually inspected to avoid using damaged or unclear tissue. Each eye was measured with Brillouin microscopy sequentially in the following order: virgin state, after LASIK flap creation, and after rapid CXL as described below. Thus, each eye served as its own control.

LASIK FLAP CREATION

LASIK flaps were created using the Amadeus II microkeratome (Ziemer USA, Alton, IL) with a 140-µm microkeratome head, blade oscillation rate of 8,000 rpm, translation speed of 2.5 mm/sec, and a 9-mm suction ring diameter, with the ML7090 (+20) CLB microkeratome blades (Med-Logics, Inc., Athens, TX). A single drop of proparacaine hydrochloride ophthalmic solution 0.5% (Akorn Pharmaceuticals, Lake Forest, IL) was applied to facilitate the microkeratome pass and minimize the risk of epithelial defect formation, which could compromise Brillouin measurements.

CXL PROCEDURE

The experiment was designed to simulate the parameters reported for the rapid CXL procedure that has been combined with LASIK in the clinical setting using parameters identical to those set out by the manufacturer and to previous reports.[12] Immediately after Brillouin measurement of the cornea following flap creation, cross-linking was performed. The flap was gently reflected and riboflavin phosphate 2.8 mg/mL (0.22% Riboflavin, Saline, Isotonic, VibeX-Xtra; Avedro, Waltham, MA) was applied to the stromal bed and soaked for 60 seconds under a low magnification light microscope. Care was taken to avoid riboflavin contact with the flap. After 60 seconds, excess riboflavin was gently rinsed off the stromal bed and the flap was repositioned in place. The cornea was then irradiated with UV-A light (CS2010 LED spot UV curing system; Thorlabs GmbH, Newton, NJ) at 30 mW/cm^2 for 80 seconds (total fluence: 2.4 J/cm^2).

BRILLOUIN CONFOCAL MICROSCOPE

The confocal Brillouin microscope used in this study has been described elsewhere (**Figure A**, available in the online version of this article).[27-30] Briefly, the system used a 532-nm laser with an optical power on the sample of 10 mW. The laser light was focused by the objective lens 20× with a numerical aperture of 0.4 (LMPLFLN; Olympus Corporation, Tokyo, Japan). The resolution was 1 µm laterally (x-y) and 5 µm axially (z). X-Z sectional images were obtained by translating with exposure time of 0.1 second. The Brillouin scattered light collected in epi-detection was spectrally analyzed by a two-stage virtually imaged phase array spectrometer and imaged onto an electron multiplication charged coupled device (CCD) camera (IXon Du-897; Andor, Belfast, Northern Ireland). Raw

data acquired by the camera were fitted with Lorentzian function to determine Brillouin frequency shifts. De-ionized water and the bottle glass with known Brillouin frequency shifts were used for the calibrations of the spectral dispersion and the free spectral range of the spectrometer. For data acquisition, we used LabVIEW (National Instruments, Austin, TX) to control motorized stages (Prior Scientific, Inc., Rockland, MA) and the CCD camera.

BRILLOUIN SHIFT RELATION TO ELASTIC MODULUS

By detecting the Brillouin frequency shift, the local mechanical properties of the material could be estimated. Specifically, the Brillouin frequency shift of the scattering photons could be related to the longitudinal elastic modulus of the material as:

$$\upsilon_B = \pm \frac{2n}{\lambda} \sqrt{\frac{M'}{\rho}} \cos\left(\frac{\theta}{2}\right)$$

in which υ_B is the Brillouin frequency shift of the scattering photons, n is the refractive index of the material, λ is the wavelength of the incident photons, M' is longitudinal elastic modulus, ρ is the density of the material, and θ is the angle between incident and the scattered photons. The refractive index and density are spatially varying[31,32]; however, the relationship between refractive index and density is linear in biological cells and tissue including cornea and follows the Gladstone–Dale relationship.[33] Thus, the ratio of ρ/n^2 is found to be approximately constant with a value of 0.57 g/cm^3 and a variation of less than 0.3% throughout the cornea.[34,35] In crystalline material and at a low frequency, the relationship between the longitudinal modulus M' and the Young's modulus E' can be expressed as $M' = E'\,(1 - \sigma)\,/\,(1 + \sigma)\,(1 - 2\sigma)$, where σ is the Poisson's ratio. However, in the Brillouin measurements, the modulus M' is in the hypersonic frequency range of 5 to 10 GHz. It has been shown empirically that the Brillouin-measured longitudinal modulus M' and the conventional Young's (or shear) modulus E' is a log-log linear relationship: $\log(M') = a\,log(E') + b$, where a and b are material-dependent coefficients.[36] The relative change can be further expressed as $\Delta M\,/\,M = a\,\Delta E\,/\,E$, thus allowing an estimation of the mechanical outcome of CXL procedures in terms of traditional elastic moduli.[24]

BRILLOUIN MEASUREMENTS

In this study, the cross-sectional scanning pattern (XZ) was used to image the cornea samples. The size of the scanning image was 1,000 µm (lateral) × 2,000 µm (axial). The eye was laid on a chamber holder with a single drop of proparacaine hydrochloride ophthalmic solution covering the corneal surface. The virgin cornea was imaged by Brillouin microscopy first. Then the LASIK flap was created as described above and the cornea was re-imaged. Following the LASIK flap, rapid CXL was performed as described above and the cornea re-imaged.

To quantify corneal modulus, the depth profiles of the Brillouin shifts were computed by averaging over the transverse axis over a range of approximately 200 µm. The profiles of the virgin state, after LASIK flap, and after rapid CXL were then normalized to the thickness of the virgin cornea for reliable comparison. Three depth regions were evaluated: anterior (80 to 180 µm), central (200 to 300 µm), and posterior cornea (300 to 500 µm).

STATISTICAL ANALYSIS

In planning the study, we estimated the number of samples to investigate based on previous literature data. For the comparison of virgin versus flap-cut corneas, an estimated decrease of 31% and 40% to 70% was reported[5,37]; for the comparison of flap-cut versus CXL corneas, an increased rigidity of approximately 130% was reported.[10] These data correspond to a target Brillouin change of approximately 40 MHz. Considering that our previous standard deviation within comparable ex vivo CXL measurements was approximately 20 MHz,[24] we expected that six samples per group would be sufficient to find a statistically significant change with power (0.9) and family-wise type I error (0.05) for two comparisons in a paired analysis. Although it would have been interesting to take a measurement for each sample at each of the three stages of the study, experimentally this was sometimes not possible (eg, some samples were physically ruined during procedures, the instrument was not ready to measure at the specific time needed, or the area of the sample was not chosen properly at the first attempt, which threw off critical timing of the experiments); our experimental design featuring two separate comparisons reflects this consideration. In the experiment, we collected nine pairs of data to compare the virgin versus flap-cut groups and seven pairs of data to compare the flap-cut versus CXL groups. The Brillouin shift differences between virgin, after LASIK flap, and after rapid CXL states were compared using both whole corneal and regional corneal thickness regions. Because of the small sample size and because not all parameters in all conditions were normally distributed, we used the non-parametric Wilcoxon signed-rank test for all comparisons, with
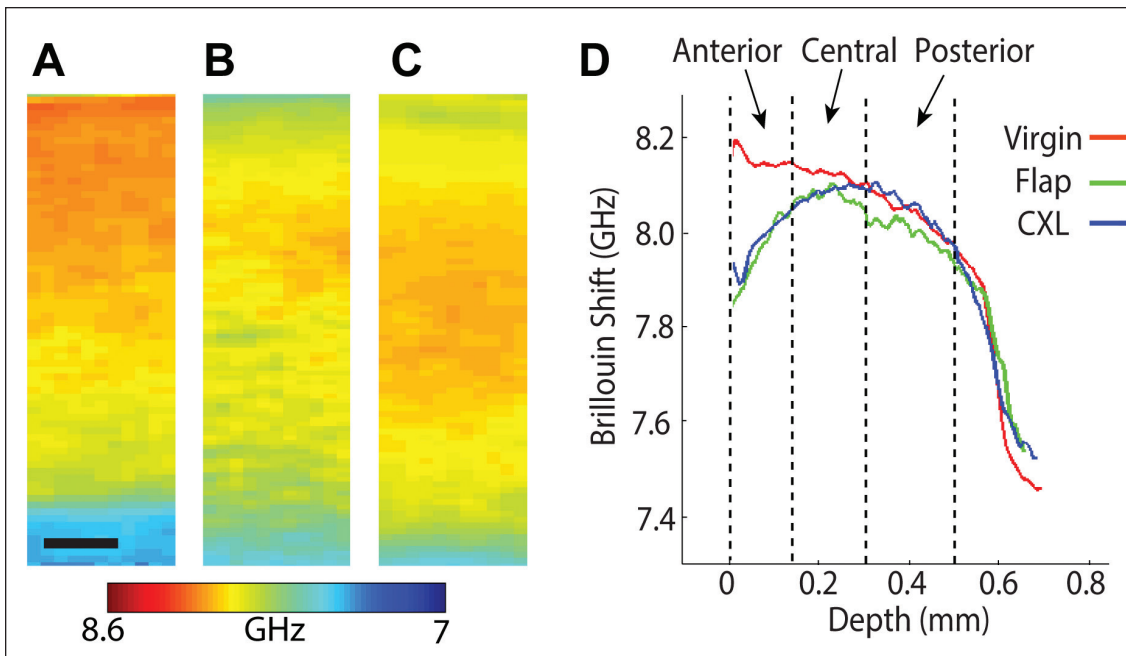
Figure 1. Brillouin shift characterization of the LASIK flap creation and rapid corneal cross-linking (CXL) procedure. (A) Representative cross-sectional Brillouin image of virgin porcine cornea. (B) Brillouin image of cornea after flap cut by LASIK flap creation. (C) Brillouin image of cornea after rapid CXL. (D) Brillouin depth profiles of the virgin cornea, after LASIK flap creation, and after rapid CXL. Scale bars are 100 μm.

a significance level adjusted to 0.025 by Bonferroni correction for two multiple comparisons.

RESULTS

A total of 11 eyes were evaluated by Brillouin imaging. To summarize the results, we computed the mean values of the Brillouin shifts for full thickness and anterior, central, and posterior cornea.

Figure 1 shows representative cross-sectional Brillouin images and Brillouin depth profile measurements in the virgin state, after LASIK flap creation, and after rapid CXL. Brillouin imaging of the virgin cornea (**Figure 1A**) showed spatially distinct Brillouin frequency shifts, which revealed the varying elastic modulus of cornea throughout the depth consistent with previous measurements.[19] Brillouin shifts were highest, corresponding to highest corneal strength, in the anterior part of the cornea and decreasing toward the endothelium, with the aqueous humor showing values close to water. After LASIK flap creation (**Figure 1B**), the Brillouin shifts in the anterior and central regions showed a marked reduction. The Brillouin shift in the posterior flap-cut cornea also decreased but much less than the anterior and central regions. After rapid CXL (**Figure 1C**), the Brillouin shift was similar to that after LASIK flap creation throughout the entire thickness of the cornea.

Figure B (available in the online version of this article) shows specific results obtained for each corneal specimen: total thickness, anterior, central, and posterior cornea. A large variation in Brillouin shift across the various samples was noticeable in the virgin state because the porcine eyes were of different ages; how-

ever, this variability did not affect our comparative analysis because each eye served as its own control.

EFFECT OF LASIK FLAP CREATION ON BRILLOUIN SHIFT

Figure 2 and **Table 1** show the comparison of Brillouin shifts in flap-cut corneas compared to virgin corneas. Because each cornea served as its own control, we plotted the differences between virgin state and after LASIK flap creation. We found a statistically significant decrease of the Brillouin shifts, denoting a statistically significant weakening due to LASIK flap creation. The decrease in Brillouin shift was significant when comparing full thickness and the anterior stromal region. The change in the mid and posterior stroma strength after LASIK flap creation was not statistically significant. As expected, the largest reduction in strength occurred in the anterior region, where the flap cut occurred.

EFFECT OF RAPID CXL AFTER LASIK FLAP CREATION ON BRILLOUIN SHIFT

Figure 3 and **Table 2** show the comparison of Brillouin shifts after LASIK flap creation and after rapid CXL. Because each cornea served as its own control, we plotted the differences between these conditions. Although the Brillouin shift was slightly higher after rapid CXL, there was no statistically significant difference in strength at any level of the corneas.

DISCUSSION

We found that significant weakening occurred in the anterior and central cornea after LASIK flap creation. Although this corneal strength reduction after LASIK
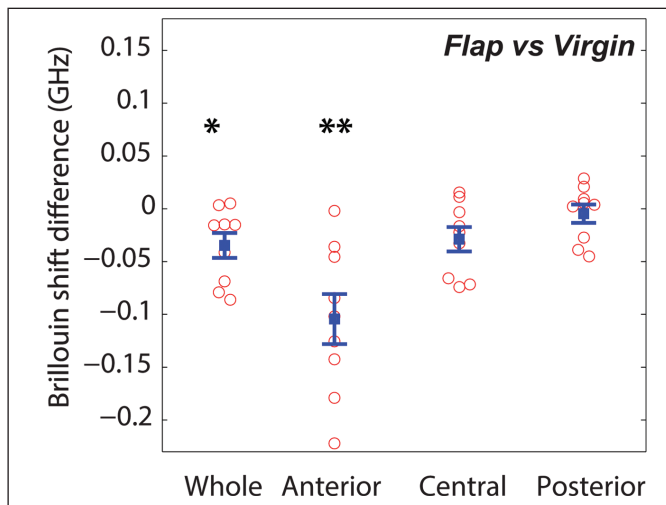
Figure 2. The differences of the mean Brillouin shifts between flap and virgin cornea (flap vs virgin) at the full thickness and three depths were plotted. Red circles were the data points. Blue squares were the mean values. The error bar was the standard error of the mean. Wilcoxon signed-rank test was used. *$P < .025$. **$P < .005$.
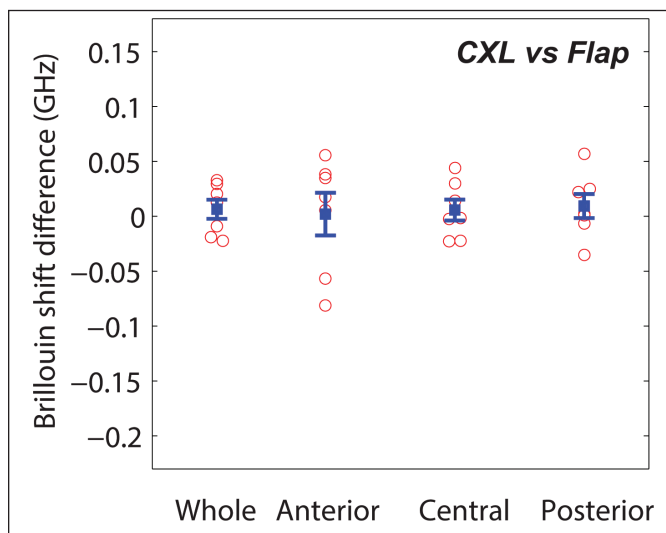

Figure 3. The differences of the mean Brillouin shifts after LASIK flap creation and after rapid cross-linking (CXL) (CXL vs Flap) at full thickness and three depths were plotted. Red circles were the data points. Blue squares were the mean values. The error bar was the standard error of the mean. Wilcoxon signed-rank test was used. No significant difference from zero was found for CXL flap overall or at any depth.

has been assumed for some time, to date these evaluations have been limited to hysteresis measurement or finite element modeling.[5]

We found that rapid CXL had minimal impact on the overall corneal stiffness after LASIK flap creation at any stromal depth.

Using the previously established log-log relationship, we could calculate the mechanical impact of the various procedures we analyzed in terms of tradi-

TABLE 1

Difference in the Brillouin Shift (GHz) Between LASIK Flap and Virgin Cornea for All Regions

Region	Mean (GHz)	SEM (GHz)	P^a
Full thickness	-0.035	0.012	.0195
Anterior	-0.104	0.024	.0039
Central	-0.029	0.012	.0391
Posterior	-0.005	0.009	.99

SEM = standard error of the mean
[a]Wilcoxon signed-rank test.

TABLE 2

Difference in the Brillouin Shift (GHz) Between Cross-linking and LASIK Flap Corneas at All Regions (n = 7)

Regions	Mean (GHz)	SEM (GHz)	P^a
Full thickness	0.006	0.009	.4688
Anterior	0.002	0.019	.9375
Central	0.006	0.010	.8125
Posterior	0.009	0.011	.4688

SEM = standard error of the mean
[a]Wilcoxon signed-rank test.

tional moduli. Our comparison of flap-cut and virgin corneas showed that the Brillouin shifts significantly decreased by approximately 35 MHz, corresponding to a Young's modulus reduction of approximately 26% after the LASIK flap creation. This is consistent with previous results. Reinstein et al.[5] estimated that postoperative total corneal tensile strength would be decreased by 31% after LASIK (110-µm flap, 400-µm residual stromal bed depth, 40-µm ablation depth) and previous modeling studies suggest 40% to 70% reduction in overall corneal modulus after LASIK, including flap cutting and stromal ablation.[5,37] Beyond previous studies, our results show that the majority of the loss of strength is concentrated in the anterior portion of the stroma, with a reduction of approximately 100 MHz (ie, a nearly 80% reduction in Young's modulus), whereas the reduction is approximately 22% in the central stroma and is less than 4% below the instrument sensitivity in the posterior stroma.

Results of the clinical and mechanical efficacy of rapid CXL combined with LASIK have provided mixed values.[38,39] In the only study that directly evaluated mechanical stiffening after CXL, Kanellopoulos et al.[10] found the rigidity of the underlying corneal stroma increased 130% by measuring the shear modulus and there was no impact on the flap of 8 human

myopic eyes ex vivo after the LASIK flap creation and rapid CXL. Based on these previous results and the previously calculated relationship between Brillouin measurements and Young's modulus, we would have expected to find an approximately 40-MHz increase in Brillouin shift, which is clearly within our instrument sensitivity; however, we found a smaller stiffening effect that was not statistically significant and close to the instrumental uncertainty (approximately 10 MHz).

Tissue hydration affects Brillouin measurements and must be accounted for when interpreting results. In separate experiments,[40] it was found that increasing corneal hydration within the physiological range causes a drop of approximately 20 MHz per 1% water content in Brillouin shift. However, the hydration-driven change in Brillouin shift due to modulus decrease is much larger than the change due to combined index-density term $n / \sqrt{\rho}$. Additionally, we reviewed corneal thickness at all steps during the experimental protocol (**Figures 1A-1C**) and could not identify a consistent or statistically significant trend in shrinking or swelling of tissue samples, which indicated that hydration effects were not prominent in our experiments.

Limitations in our study include a small sample size, working with porcine corneas instead of human eyes, and a LASIK case simulation without actual ablation. Porcine models have been used extensively for cross-linking research.[15,16] LASIK flap creation is the most biomechanically impactful step in the LASIK procedure[42]; thus, we believe this simulation was appropriate to test what we set out to evaluate. Further, because we used each eye as its own control, rapid CXL should have had a comparatively equivalent effect with or without excimer laser stromal ablation.

We found that LASIK flap creation significantly reduces overall corneal strength, particularly within the anterior and central corneal stromal regions. The application of rapid CXL provided no significant stiffening effect. Future studies with Brillouin microscopy could provide the non-invasive assessment of the mechanical outcome of refractive and cross-linking procedures in vivo.

AUTHOR CONTRIBUTIONS

REFERENCES

1. Randleman JB, Woodward M, Lynn MJ, Stulting RD. Risk assessment for ectasia after corneal refractive surgery. *Ophthalmology*. 2008;115:37-50.

2. Santhiago MR, Smadja D, Gomes BF, et al. Association between the percent tissue altered and post-laser in situ keratomileusis ectasia in eyes with normal preoperative topography. *Am J Ophthalmol*. 2014;158:87-95.

3. Reinstein DZ, Archer TJ, Urs R, Gobbe M, RoyChoudhury A, Silverman RH. Detection of keratoconus in clinically and algorithmically topographically normal fellow eyes using epithelial thickness analysis. *J Refract Surg*. 2015;31:736-744.

4. Sinha Roy A, Dupps WJ Jr, Roberts CJ. Comparison of biomechanical effects of small-incision lenticule extraction and laser in situ keratomileusis: finite-element analysis. *J Cataract Refract Surg*. 2014;40:971-980.

5. Reinstein DZ, Archer TJ, Randleman JB. Mathematical model to compare the relative tensile strength of the cornea after PRK, LASIK, and small incision lenticule extraction. *J Refract Surg*. 2013;29:454-460.

6. Wollensak G, Spoerl E, Seiler T. Riboflavin/ultraviolet-a-induced collagen crosslinking for the treatment of keratoconus. *Am J Ophthalmol*. 2003;135:620-627.

7. Randleman JB, Khandelwal SS, Hafezi F. Corneal cross-linking. *Surv Ophthalmol*. 2015;60:509-523.

8. Kymionis GD, Tsoulnaras KI, Liakopoulos DA, Skatharoudi CA, Grentzelos MA, Tsakalis NG. Corneal stromal demarcation line depth following standard and a modified high intensity corneal cross-linking protocol. *J Refract Surg*. 2016;32:218-222.

9. Peyman A, Nouralishahi A, Hafezi F, Kling S, Peyman M. Stromal demarcation line in pulsed versus continuous light accelerated corneal cross-linking for keratoconus. *J Refract Surg*. 2016;32:206-208.

10. Kanellopoulos AJ, Asimellis G, Salvador-Culla B, Chodosh J, Ciolino JB. High-irradiance CXL combined with myopic LASIK: flap and residual stroma biomechanical properties studied ex vivo. *Br J Ophthalmol*. 2015;99:870-874.

11. Randleman JB, Dawson DG, Grossniklaus HE, McCarey BE, Edelhauser HF. Depth-dependent cohesive tensile strength in human donor corneas: implications for refractive surgery. *J Refract Surg*. 2008;24:s85-89.

12. Kanellopoulos AJ. Long-term safety and efficacy follow-up of prophylactic higher fluence collagen cross-linking in high myopic laser-assisted in situ keratomileusis. *Clin Ophthalmol*. 2012;6:1125-1130.

13. Seiler TG, Fischinger I, Koller T, Derhartunian V, Seiler T. Superficial corneal crosslinking during laser in situ keratomileusis. *J Cataract Refract Surg*. 2015;41:2165-2170.

14. Chan TC, Yu MC, Ng AL, et al. Short-term variance of refractive outcomes after simultaneous LASIK and high-fluence crosslinking in high myopic correction. *J Refract Surg*. 2016;32:664-670.

15. Wollensak G, Spoerl E. Collagen crosslinking of human and porcine sclera. *J Cataract Refract Surg*. 2004;30:689-695.

16. Wollensak G, Spoerl E, Seiler T. Stress-strain measurements of human and porcine corneas after riboflavin-ultraviolet-A-induced cross-linking. *J Cataract Refract Surg*. 2003;29:1780-1785.

17. Scarcelli G, Yun SH. In vivo Brillouin optical microscopy of the human eye. *Opt Express*. 2012;20:9197-9202.

18. Girard MJ, Dupps WJ, Baskaran M, et al. Translating ocular biomechanics into clinical practice: current state and future prospects. *Curr Eye Res*. 2015;40:1-18.

19. Scarcelli G, Pineda R, Yun S. Brillouin optical microscopy for corneal biomechanics. *Invest Ophthalmol Vis Sci*. 2012;53:185-190.

20. Scarcelli G, Besner S, Pineda R, Kalout P, Yun SH. In vivo biomechanical mapping of normal and keratoconus corneas. *JAMA Ophthalmol*. 2015;133:480-482.

21. Scarcelli G, Besner S, Pineda R, Yun S. Biomechanical characterization of keratoconus corneas ex vivo with Brillouin microscopy. *Invest Ophthalmol Vis Sci*. 2014;55:4490-4495.

22. Kwok SJJ, Kuznetsov IA, Kim M, Choi M, Scarcelli G, Yun SH. Selective two-photon collagen crosslinking in situ measured by Brillouin microscopy. *Optica*. 2016;3:469-472.

23. Cherfan D, Verter EE, Melki S, et al. Collagen cross-linking using rose bengal and green light to increase corneal stiffness. *Invest Ophthalmol Vis Sci*. 2013;54:3426-3433.

24. Scarcelli G, Kling S, Quijano E, Pineda R, Marcos S, Yun SH. Brillouin microscopy of collagen crosslinking: noncontact depth-dependent analysis of corneal elastic modulus. *Invest Ophthalmol Vis Sci*. 2013;54:1418-1425.

25. Shah S, Laiquzzaman M, Bhojwani R, Mantry S, Cunliffe I. Assessment of the biomechanical properties of the cornea with the ocular response analyzer in normal and keratoconic eyes. *Invest Ophthalmol Vis Sci*. 2007;48:3026-3031.

26. Hallahan KM, Rocha K, Roy A, Randleman JB, Stulting RD, Dupps WJ Jr. Effects of corneal crosslinking on ocular response analyzer waveform-derived variables in keratoconus and post-refractive surgery ectasia. *Eye Contact Lens*. 2014;40:339-344.

27. Scarcelli G, Polacheck WJ, Nia HT, et al. Noncontact three-dimensional mapping of intracellular hydromechanical properties by Brillouin microscopy. *Nat Methods*. 2015;12:1132-1134.

28. Scarcelli G, Yun SH. Multistage VIPA etalons for high-extinction parallel Brillouin spectroscopy. *Opt Express*. 2011;19:10913-10922.

29. Scarcelli G, Yun SH. Confocal Brillouin microscopy for three-dimensional mechanical imaging. *Nat Photonics*. 2008;2:39-43.

30. Scarcelli G, Kim P, Yun SH. Cross-axis cascading of spectral dispersion. *Opt Lett*. 2008;33:2979-2981.

31. Kikkawa Y, Hirayama K. Uneven swelling of corneal stroma. *Invest Ophthalmol*. 1970;9:735-741.

32. Wilson G, Oleary DJ, Vaughan W. Differential swelling in compartments of the corneal stroma. *Invest Ophthalmol Vis Sci*. 1984;25:1105-1108.

33. Leonard DW, Meek KM. Refractive indices of the collagen fibrils and extrafibrillar material of the corneal stroma. *Biophys J*. 1997;72:1382-1387.

34. He X, Liu J. A quantitative ultrasonic spectroscopy method for noninvasive determination of corneal biomechanical properties. *Invest Ophthalmol Vis Sci*. 2009;50:5148-5154.

35. Ortiz S, Siedlecki D, Grulkowski I, et al. Optical distortion correction in optical coherence tomography for quantitative ocular anterior segment by three-dimensional imaging. *Opt Express*. 2010;18:2782-2796.

36. Scarcelli G, Kim P, Yun SH. In vivo measurement of age-related stiffening in the crystalline lens by Brillouin optical microscopy. *Biophys J*. 2011;101:1539-1545.

37. Roy AS, Dupps WJ Jr. Patient-specific modeling of corneal refractive surgery outcomes and inverse estimation of elastic property changes. *J Biomech Eng*. 2011;133:011002.

38. Wernli J, Schumacher S, Spoerl E, Mrochen M. The efficacy of corneal cross-linking shows a sudden decrease with very high intensity UV light and short treatment time. *Invest Ophthalmol Vis Sci*. 2013;54:1176-1180.

39. Hammer A, Richoz O, Arba Mosquera S, Tabibian D, Hoogewoud F, Hafezi F. Corneal biomechanical properties at different corneal cross-linking (CXL) irradiances. *Invest Ophthalmol Vis Sci*. 2014;55:2881-2884.

40. Shao P, Ramier A, Behrouz T, et al. Effects of corneal hydration on Brillouin measurements. Presented at the Association for Research in Vision and Ophthalmology annual meeting; May 7-11, 2011; Baltimore, MD. Abstract no. 4323.
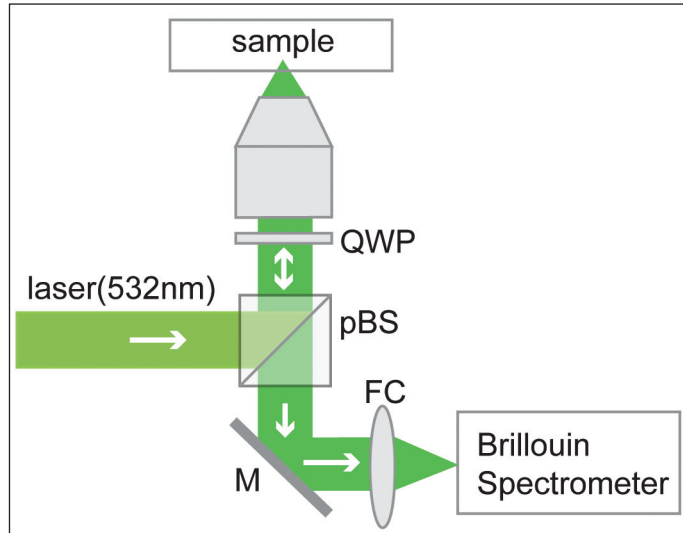
Figure A. Brillouin microscopy experimental set-up. QWP = quarter-wave plate; pBS = polarizing beam splitter; FC = fiber coupler; M = mirror
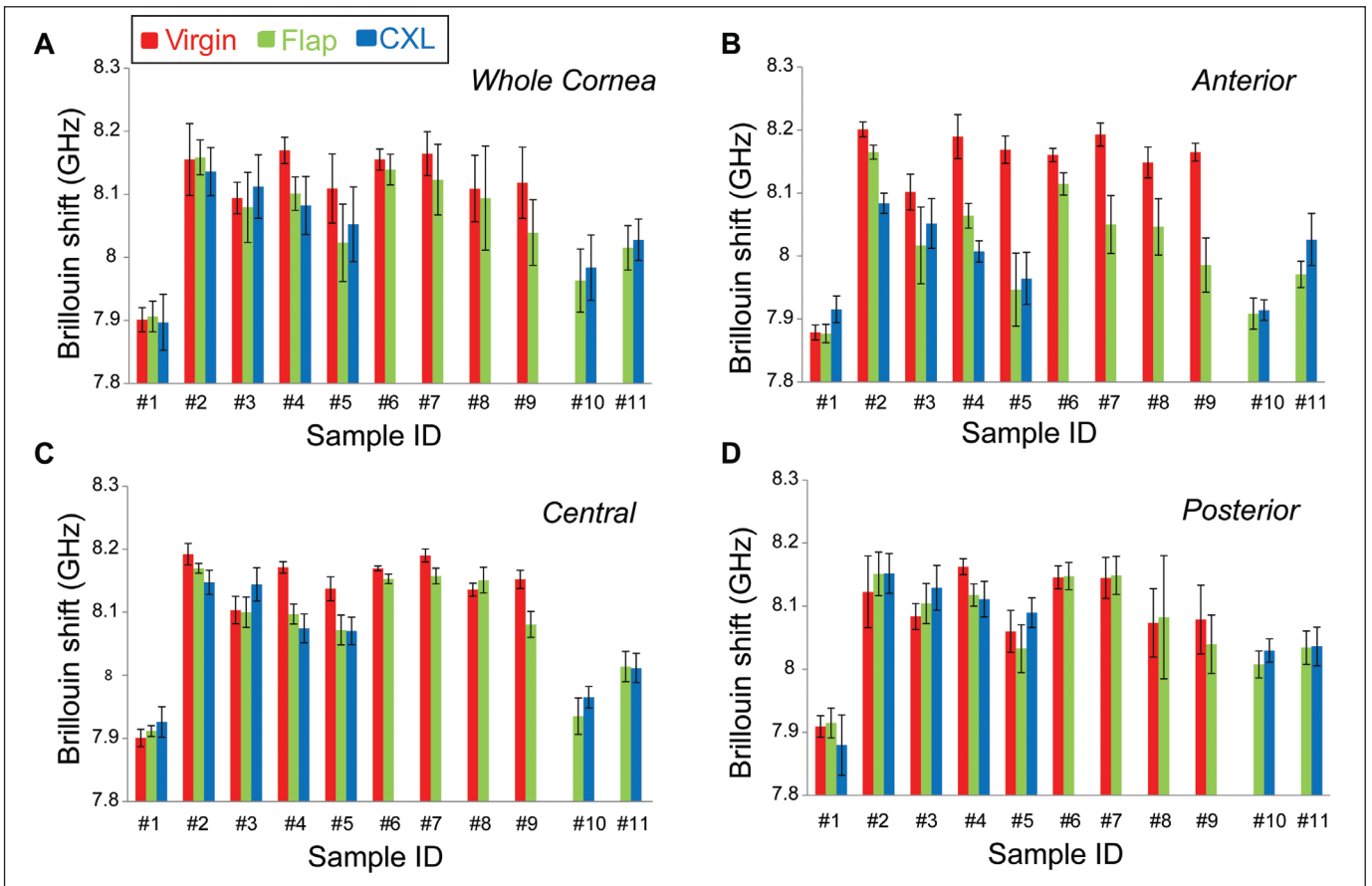

Figure B. The mean Brillouin shifts of all corneas at the full thickness and three depths were plotted. (A) Total thickness, (B) anterior (80 to 180 μm), (C) central (200 to 300 μm), and (D) posterior cornea (300 to 500 μm).